

Photon statistics and dynamics of Fluorescence Resonance Energy Transfer

Andrew J. Berglund,* Andrew C. Doherty, and Hideo Mabuchi

Norman Bridge Laboratory of Physics 12-33, California Institute of Technology, Pasadena, CA 91125

We report high time-resolution measurements of photon statistics from pairs of dye molecules coupled by fluorescence resonance energy transfer (FRET). In addition to quantum-optical photon antibunching, we observe photon bunching on a timescale of several nanoseconds. We show by numerical simulation that configuration fluctuations in the coupled fluorophore system could account for minor deviations of our data from predictions of basic Förster theory. With further characterization we believe that FRET photon statistics could provide a unique tool for studying DNA mechanics on timescales from $10^{-9} - 10^{-3}$ s.

Fluorescence Resonance Energy Transfer (FRET) has become a widespread tool for probing molecular structure and dynamics. Recent demonstrations of single-molecule sensitivity in optical assays based on FRET [1, 2] have led to significant advances in our understanding of topics such as RNA folding and ribozyme function [3]. Interpretation of FRET data generally relies on a simple physical model involving near-field dipole-dipole interactions between molecules, which was first proposed by Förster [4]. While some basic features of this model pertaining to steady-state solutions have previously been verified experimentally, dynamical details have been largely inaccessible. In this Letter, we report the use of a Hanbury-Brown Twiss apparatus to record photon statistics of the light emitted by FRET-coupled dye pairs with nanosecond resolution, and show that a careful comparison of our data with predictions of Förster theory supports the basic model but indicates a class of additional factors that must be considered. Our analysis suggests that conformational fluctuations of the substrate for the FRET-coupled dyes could be such a factor, which in turn points to the intriguing possibility of utilizing FRET photon statistics for novel assays in DNA and protein mechanics.

The FRET process involves non-radiative transfer of energy from a donor, which absorbs a photon of incident light, to an acceptor that is not directly coupled to the incident light. Detection of acceptor fluorescence is thus a simple indicator of FRET activity. A schematic energy-level diagram of molecular states is shown in Fig. 1. Under appropriate conditions of spectral overlap, Förster theory [4] predicts that the rate Γ_F of energy transfer varies as $\Gamma_F \propto \kappa^2/R^6$, where κ^2 depends on the orientation of the fluorescent species and R is the distance between them. For commonly-used organic dyes, the sensitivity of Γ_F to variations in R is greatest in the range of several nm; hence experimental determination of Γ_F yields information on distance scales relevant to biological macromolecules. The R^{-6} distance dependence of Förster theory has been experimentally confirmed using ‘ruler’ strands of DNA [1].

Intensity correlation functions of the light emitted by FRET-coupled dyes pairs carries further information about the molecular physics of FRET. The second-order

intensity correlation function (for a *stationary* process) gives the normalized time-average intensity $I_k(t + \tau)$ of mode k at time $t + \tau$ multiplied by the intensity in mode j at time t :

$$g_{jk}^{(2)}(\tau) = \frac{\langle I_j(t)I_k(t + \tau) \rangle}{\langle I_j(t) \rangle \langle I_k(t) \rangle}. \quad (1)$$

For $j = k$, this quantity is the autocorrelation of the intensity field j . Nonclassical photon statistics [5], for which $g_{jj}^{(2)}(\tau) > g_{jj}^{(2)}(0)$ for some $\tau > 0$, were first observed in an atomic beam [6]. Since then, photon antibunching has been observed in a variety of systems [7, 8, 9, 10].

We have measured $g_{jk}^{(2)}(\tau)$ for individual FRET-coupled Cy3 and Cy5 dye molecules tethered to DNA [20]. We show that our data should be sensitive not only to the mean values of FRET parameters, but also to underlying molecular processes that perturb their values on any timescale down to that of the radiative lifetimes. The techniques presented here thus provide potential experimental access to molecular dynamics that influence radiative level structures and couplings in the range 10-1000 ns, in a manner complementary to that of established techniques such as fluorescence correlation spectroscopy. Intriguing examples of such dynamics include photochemical processes, chemical shifts arising from changes in the local environment, single base-pair fluctuations in DNA secondary structure formation, and

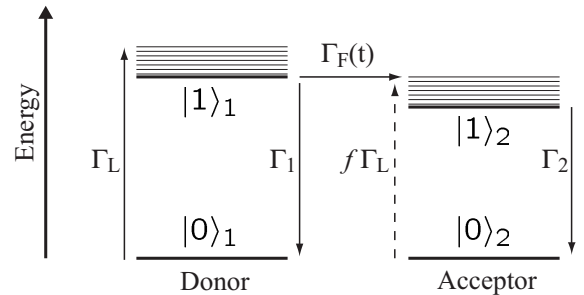


FIG. 1: Energy-level diagram of molecular states relevant to the basic Förster model. Donor states on the left are coupled by FRET to acceptor states on the right.

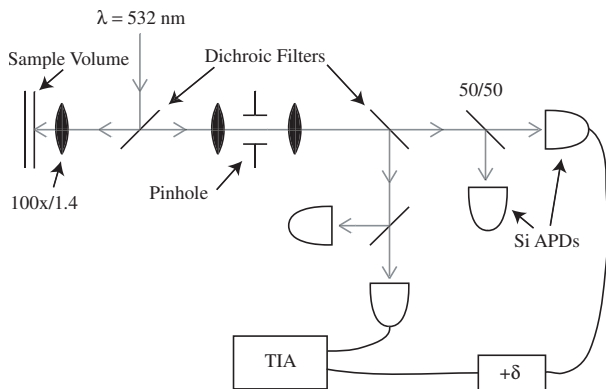


FIG. 2: Schematic diagram of the apparatus. When making cross-correlation measurements, the 50/50 beam-splitters are removed to improve collection efficiency. Spectral filters and focusing optics at the APDs are not shown.

conformational fluctuations on much shorter timescales than have previously been studied using FRET. Molecular dynamics simulations of nucleic acid mechanics are generally tractable only for integration times ~ 10 ns [11], so that experimental access to these timescales may provide fruitful contact between theory and experiment.

A diagram of our apparatus appears in Fig. 2. It consists of confocal imaging optics coupled to Hanbury Brown-Twiss (HBT) detection channels [12]. We focus $140 \mu\text{W}$ of 532 nm laser light between glass cover slips through a diffraction-limited microscope objective (Carl Zeiss). Fluorescence is collected by the same objective and imaged onto a $100 \mu\text{m}$ -diameter pinhole. A dichroic filter separates Stokes-shifted fluorescence light from scattered excitation light. A second dichroic filter separates donor fluorescence (570 nm) and acceptor fluorescence (670 nm) into separate HBT channels each containing a 50/50 beam-splitter, spectral filters and 2 avalanche photodiode single-photon counters (APDs). In each experiment, photon arrival times at one pair of detectors are recorded with sub-ns resolution by a time-interval analyzer (TIA). An electronic delay of $\delta = 50$ ns is imposed in one channel to avoid small time-interval crosstalk in the TIA.

We monitor fluorescence from dual-labelled DNA hairpins in aqueous buffer at room temperature. The donor and acceptor are tethered at complementary positions, so that they exhibit a high FRET efficiency. In a typical experiment, we place $1 \mu\text{L}$ of 1 nM dye-labelled DNA solution between the cover slips. The axial position of the microscope objective is actively locked by a piezo-electric translator so that it is stable to $\lesssim 100$ nm for periods much longer than a typical experimental run (~ 6 hrs). We choose a low enough DNA concentration that there are no molecules in the imaging volume for a large fraction of the observation time. The count rate at the detectors then shows background light punctuated by bursts of

fluorescence as individual DNA strands diffuse through the imaging volume. Since fluorescence from separate DNA strands is *uncorrelated*, the presence of multiple molecules in the imaging volume reduces the sharpness of features in the measured correlation functions.

To measure $g_{jk}^{(2)}(\tau)$, we choose a pair of detectors and histogram the time interval between photon arrivals, keeping only data for which both detection channels were active (the TIA-limited channel dead time is 243 ns). We choose a threshold count rate for each channel (the maximum expected count rate over a 1 ms interval, given the mean count rate over the ~ 1 s local measurement interval), and keep only those data for which at least one channel exceeds this threshold. In this way, we reduce the contribution from background light recorded when no molecule is present in the imaging volume. Measured correlation functions, averaged over many molecular transits, are shown in Fig. 3. The precise time delay imposed by optical and electronic path differences (the $\tau = 0$ point) is determined by measuring correlation functions of a pulsed LED.

Interpretation of the experimental results proceeds from a straightforward model for Monte Carlo simulation of this and similar experiments. The donor and acceptor are organic molecules attached to a complex substrate. Electronic excitation is followed by fast rotational and vibrational relaxation, so our model assumes negligible coherence between electronic states. We represent the donor and acceptor, labelled $j = 1, 2$ respectively, as two-level emitters with basis states $\{|0\rangle_j, |1\rangle_j\}$ (see Fig. 1) and lowering operator σ_j . Since we assume no coherent interactions, we write a master equation for the time evolution of the density operator of the system ρ with only incoherent (jump) terms:

$$\frac{\partial \rho}{\partial t} = \sum_{m=1}^M \Gamma_m(t) \left\{ \Lambda_m \rho \Lambda_m^\dagger - \frac{1}{2} (\Lambda_m^\dagger \Lambda_m \rho + \rho \Lambda_m^\dagger \Lambda_m) \right\}. \quad (2)$$

The ‘jump operators’ Λ_m and associated (possibly time-dependent) rates $\Gamma_m(t)$ represent the incoherent transitions that can occur in the system. In our case we choose $M = 5$ possible transitions, but it is straightforward to generalize the model to include more processes. These transitions are: direct excitation of the donor with rate Γ_L ; off-resonant excitation of the acceptor with rate $f\Gamma_L$, $f < 1$; donor (acceptor) spontaneous emission with rate Γ_1 (Γ_2); and FRET energy transfer from donor to acceptor excited state with time-dependent rate $\Gamma_F(t)$. A FRET transition is represented by $\Gamma_5(t) = \Gamma_F(t)$, $\Lambda_5 = \sigma_1 \otimes \sigma_2^\dagger$. The other jump operators are similarly defined. Eq. (2) is equivalent to a linear system of rate equations for the ground and excited state populations of the donor and acceptor, and can thus be solved exactly when the time-variation of all parameters is specified analytically. For stochastic parameter

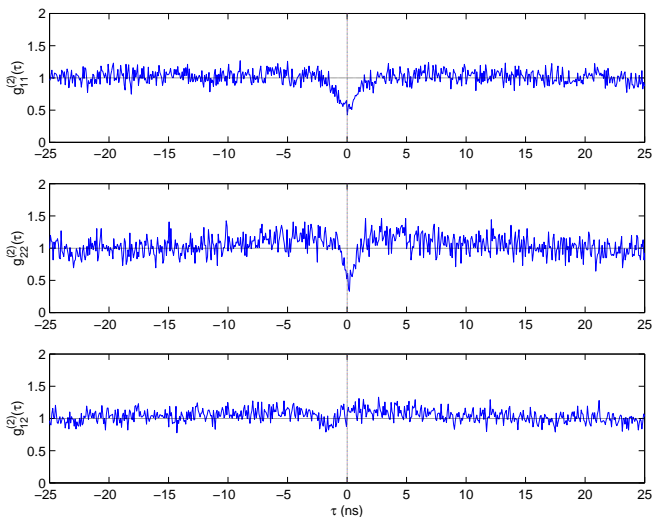


FIG. 3: Measured correlation functions for high FRET-efficiency donor-acceptor pair fluorescence. Top: donor intensity autocorrelation (partially contaminated by inactive Cy5). Middle: acceptor intensity autocorrelation. Bottom: donor-acceptor cross-correlation, the average intensity in the acceptor channel, given a photon arrival in the donor channel at $\tau = 0$. See text for a discussion of the bunching at $\sim \pm 5$ ns in the acceptor autocorrelation.

variation, we resort to numerical simulation.

The measured autocorrelation functions in Fig. 3 show pronounced antibunching dips at $\tau = 0$. For a *single* fluorophore, $g_{jj}^{(2)}(0) = 0$ since two photons (in the same mode) can never be emitted simultaneously, *i.e.*, in a time-interval $\tau = 0$. The observed value of $g_{jj}^{(2)}(0)$ is a function *only* of the signal-to-noise ratio S at each detector and the probability $P(N)$ that N molecules are observed simultaneously. In order to understand the depth of the $\tau = 0$ minimum in the autocorrelation functions, we make independent estimates of $P(N)$ and S . Neglecting crosstalk between channels and assuming Poisson-distributed background, it can be shown from (1) that

$$g_{jj}^{(2)}(0) = 1 - \sum_{N \geq 1} P(N) \frac{1}{\nu_j(N)} \quad (3)$$

$$\nu_j(N) = N + \left(\frac{1}{S_j^{(1)}} + \frac{1}{S_j^{(2)}} \right) + \frac{1}{N S_j^{(1)} S_j^{(2)}} \quad (4)$$

where $S_j^{(n)}$ is the signal-to-noise ratio of HBT arm n , mode j . Assuming $P(N)$ is a Poisson distribution with mean value $\langle N \rangle$, we determine the fraction of all photodetection events attributed to molecular fluorescence (*i.e.*, exceeding the threshold count rate criterion described above). This fraction is $\sum_{N \geq 1} P(N)$ from which we can solve for $\langle N \rangle$. For a typical run, we estimate $\langle N \rangle \approx 0.1$ in this way. The probability that $N \geq 2$ molecules are observed is therefore < 0.005 so that we are firmly in the single-molecule regime. We estimate the

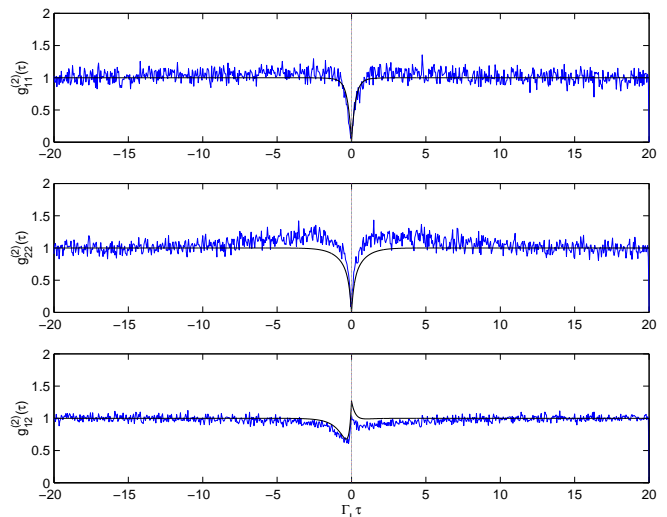


FIG. 4: Monte Carlo calculation of correlation functions for a jump-process Förster transfer rate with correlation time $\tau_F = 7$. Top: donor intensity autocorrelation. Middle: acceptor intensity autocorrelation. Bottom: donor-acceptor cross-correlation. The smooth curves are deterministic simulations with fixed $\Gamma_F(t) = \langle \Gamma_F \rangle$. The parameters used were $\Gamma_1 = \Gamma_2 = 1$, $\Gamma_F^H = 10$, $\Gamma_F^L = 0$, $f = 0.1$. All rates (times) are in units of the laser excitation rate Γ_L ($1/\Gamma_L$).

signal-to-noise ratios $S_j^{(n)}$ by comparing the fluorescence count rate to the background count rate. A typical value is $S \approx 5$. From signal-to-noise and image volume occupancy statistics, we expect $g_{11}^{(2)}(0) = 0.23$ for the donor and $g_{22}^{(2)}(0) = 0.32$ for the acceptor autocorrelation.

In our experiment, we see a large fraction ($\sim 60\%$) of low FRET-efficiency events, indicating a subpopulation of fluorophores exhibiting little or no FRET coupling. These events, which we attribute to acceptor photobleaching, contribute a background that contaminates the shape of $g_{11}^{(2)}(\tau)$. [In this experiment, we are limited by the TIA to time-resolution on two detectors only and are thus unable to exclude FRET-inactive dye pairs when measuring $g_{11}^{(2)}(\tau)$.] Both the cross-correlation and acceptor autocorrelation depend on *acceptor* fluorescence events, and are therefore robust against a bare-donor subpopulation. The depth of the observed $\tau = 0$ feature in the acceptor autocorrelation is consistent with our independent estimate based on signal-to-background and image volume occupancy statistics.

In addition to photon antibunching on radiative timescales, we see bunching ($g_{22}^{(2)}(\tau) > 1$) at longer time intervals (~ 5 ns) in the acceptor autocorrelation of Fig. 3. This bunching indicates clustering of acceptor events on the same timescale, most likely arising from fluctuations in $\Gamma_F(t)$. We expect that our fluorophores rotate with a characteristic time of ~ 250 ps, so rotational diffusion is an unlikely explanation for the observed correlations [13]. Numerical simulations investigating the influence of rota-

tional diffusion on $\Gamma_F(t)$ do not reproduce the features in our data. We rather suspect FRET ‘intermittency’, possibly related to fast diffusion of tethered dye molecules and their propensity to stick to DNA [14, 15]. Intersystem crossing and spectral diffusion for fluorophores such as Cy5 are known to exhibit longer timescales [16, 17].

We model FRET intermittency by allowing $\Gamma_F(t)$ to jump between a high value Γ_F^H and a low value Γ_F^L (as perhaps when one or both dyes are stuck to the DNA) with a correlation time τ_F . Numerical results are shown in Fig. 4, where we see antibunching followed by bunching at τ_F [21]. Deterministic simulations (smooth curves) with fixed $\Gamma_F(t)$ do not exhibit bunching in the acceptor autocorrelation. Most calculated and observed features are consistent with intuition based on the four-level model. Under conditions of high FRET efficiency, donor emission rarely occurs. However, for a sufficiently strong driving field, the excitation rate is large compared to the acceptor emission rate, and donor absorption may occur when the acceptor is already in its excited state. In this ‘exciton blockade’ situation, FRET cannot occur since the acceptor is already excited. Subsequent donor emission is highly probable followed by acceptor emission a short time later. The conditional probability for acceptor fluorescence is therefore enhanced by observation of a donor emission event, which is represented by a cusp at short positive times in the cross-correlation. The dip in the cross-correlation at negative τ can be understood in a similar way. Observation of an acceptor photon *deterministically* prepares the acceptor in its ground state. Since the acceptor is in its ground state, FRET occurs with high probability since any residual donor excitation is efficiently transferred to the acceptor. This depressed probability for donor fluorescence at short times after acceptor fluorescence is represented by a dip at negative τ in the cross-correlation. Cross-correlations exhibiting other types of conditional statistics have been observed in cascaded multi-exciton emission from semiconductor quantum dots. [18, 19].

In summary, we have measured FRET photon statistics and presented an intuitive model for interpretation of such experiments. Our data are in basic agreement with simple Förster theory, but the shape of the acceptor autocorrelation is strongly suggestive of additional dynamics at ~ 5 ns timescales. Numerical simulations show that this inconsistency is resolved by the inclusion of stochastic variations in the donor-acceptor coupling strength. We have suggested a possible molecular mechanism for these fluctuations, but further experiments are necessary to characterize the biochemical details.

Our model suggests that thermally excited bending modes of dye-labelled, rod-like molecules should be vis-

ible in $g_{jk}^{(2)}(\tau)$ for appropriate motional amplitudes and timescales. We hope to exploit this dependence in studying the conformational dynamics of semi-rigid DNA and synthetic proteins. Furthermore, future experiments incorporating direct excitation of the acceptor fluorophore will allow absolute determination of model parameters. We believe these techniques can be developed into an important new optical single-molecule method for characterization of macromolecular dynamics on nanosecond (and longer) timescales.

The authors thank E. Winfree, R. Phillips, and X. Zhuang for informative discussions, and T. McGarvey for technical assistance. This research was supported by the NSF under grant EIA-0113443 and by the W. M. Keck Discovery Fund. A. B. acknowledges the support of an NSF Graduate Fellowship.

* Electronic address: berglund@caltech.edu

- [1] A. A. Deniz *et al.*, Proc. Natl. Acad. Sci. USA **96**, 3670 (1999).
- [2] T. Ha *et al.*, Proc. Natl. Acad. Sci. USA **96**, 9077 (1999).
- [3] S. Weiss, Nat. Struct. Biol. **7**, 724 (2000).
- [4] T. Förster, Ann. Phys. **2**, 55 (1948).
- [5] L. Mandel and E. Wolf, *Optical Coherence and Quantum Optics* (Cambridge University Press, 1995).
- [6] H. J. Kimble, M. Dagenais, and L. Mandel, Phys. Rev. Lett. **39**, 691 (1977).
- [7] P. Kask, P. Piksarv, and U. Mets, Eur. Biophys. J. **12**, 163 (1985).
- [8] F. Diedrich and H. Walther, Phys. Rev. Lett. **58**, 203 (1987).
- [9] P. Michler *et al.*, Nature **406**, 968 (2000).
- [10] L. Fleury *et al.*, Phys. Rev. Lett. **84**, 1148 (2000).
- [11] T. E. Cheatham III and P. A. Kollman, Annu. Rev. Phys. Chem. **51**, 435 (2000).
- [12] R. Hanbury Brown and R. Q. Twiss, Nature **178**, 1447 (1956).
- [13] T. Ha *et al.*, J. Phys. Chem. B **103**, 6839 (1999).
- [14] L. Edman, U. Mets, and R. Rigler, Proc. Natl. Acad. Sci. USA **93**, 6710 (1996).
- [15] D. G. Norman *et al.*, Biochemistry **39**, 6317 (2000).
- [16] J. Bernard *et al.*, J. Chem. Phys. **98**, 850 (1993).
- [17] P. Tinnefeld, D.-P. Herten, and M. Sauer, J. Phys. Chem. A **105**, 7989 (2001).
- [18] D. V. Regelman *et al.*, Phys. Rev. Lett. **87**, 257401 (2001).
- [19] A. Kiraz *et al.*, Phys. Rev. B **65**, 161303 (2002).
- [20] Integrated DNA Technologies molecular beacons.
- [21] For this ‘random telegraph’ process, the model is analytically solvable. We emphasize that the Monte Carlo techniques presented here may be used to simulate parameter variation with arbitrary statistics.